

This is a repository copy of *Performance of coherent-state quantum target detection in the context of asymmetric hypothesis testing*.

White Rose Research Online URL for this paper:

<https://eprints.whiterose.ac.uk/184539/>

Version: Accepted Version

---

**Article:**

Spedalieri, Gaetana and Pirandola, Stefano orcid.org/0000-0001-6165-5615 (2022)  
Performance of coherent-state quantum target detection in the context of asymmetric hypothesis testing. IET Quantum Communication. ISSN 2632-8925

<https://doi.org/10.1049/qtc2.12036>

---

**Reuse**

Items deposited in White Rose Research Online are protected by copyright, with all rights reserved unless indicated otherwise. They may be downloaded and/or printed for private study, or other acts as permitted by national copyright laws. The publisher or other rights holders may allow further reproduction and re-use of the full text version. This is indicated by the licence information on the White Rose Research Online record for the item.

**Takedown**

If you consider content in White Rose Research Online to be in breach of UK law, please notify us by emailing [eprints@whiterose.ac.uk](mailto:eprints@whiterose.ac.uk) including the URL of the record and the reason for the withdrawal request.

# Performance of coherent-state quantum target detection in the context of asymmetric hypothesis testing

Gaetana Spedalieri and Stefano Pirandola

*Department of Computer Science, University of York, York YO10 5GH, UK*

Due to the difficulties of implementing joint measurements, quantum illumination schemes that are based on signal-idler entanglement are difficult to implement in practice. For this reason, one may consider quantum-inspired designs of quantum lidar/radar where the input sources are semiclassical (coherent states) while retaining the quantum aspects of the detection. The performance of these designs could be studied in the context of asymmetric hypothesis testing by resorting to the quantum Stein's lemma. However, here we discuss that, for typical finite-size regimes, the second- and third-order expansions associated with this approach are not sufficient to prove quantum advantage.

## Introduction

In coherent-state quantum target detection one exploits a semiclassical source, specifically coherent states but a quantum detection scheme, not necessarily homodyne or heterodyne detection (which are used classically [1]). This can therefore be considered a quantum-inspired radar (QIR) since we relax the quantum properties of the transmitter (i.e. no use of entanglement as in quantum illumination [2–6]) while retaining the optimal quantum performance of the receiver. We assume the single-bin setting which corresponds to looking at some fixed range  $R$  and solving a binary test of target absent (null hypothesis  $H_0$ ) or present (alternative hypothesis  $H_1$ ). We perform our study in the setting of asymmetric hypothesis testing [7–10], so that we fix the false-alarm probability to some reasonably low value, e.g.,  $p_{\text{FA}} = 10^{-5}$ , and then we minimize the probability of mis-detection  $p_{\text{MD}}$ . Thus we look at the performance in terms of mis-detection probability  $p_{\text{MD}}$  versus signal-to-noise ratio (SNR)  $\gamma$ .

More precisely, these are the two quantum hypotheses to discriminate:

$\mathbf{H}_0$ : A completely thermalizing channel, i.e., a channel with zero transmissivity in an environment with  $\bar{n}_B$  mean thermal photons (target absent).

$\mathbf{H}_1$ : A lossy channel with transmissivity  $\eta$  and thermal noise  $\bar{n}_B/(1-\eta)$ , where the re-scaling avoids the possibility of a passive signature (target present).

Let us consider an input coherent state  $|\alpha\rangle$  with mean number of photons  $\bar{n}_S = |\alpha|^2$  and mean value  $\bar{\mathbf{x}}_S = (\bar{q}, \bar{p})^T = \sqrt{2}(\text{Re } \alpha, \text{Im } \alpha)^T$ . Without losing generality, we can assume that  $\alpha$  is real, so that  $\bar{\mathbf{x}}_S = (\bar{q}, \bar{p})^T = \sqrt{2}(\alpha, 0)^T$ . On reflection from the potential target, we have two possible output states:

$\mathbf{H}_0$ : A thermal state  $\rho_0^{\text{th}}$  with zero mean  $\bar{\mathbf{x}}_0 = 0$  and covariance matrix (CM)  $\mathbf{V}_0 = (\bar{n}_B + 1/2)\mathbf{I}$ .

$\mathbf{H}_1$ : A displaced thermal state  $\rho_1^{\text{th}}$  with mean value  $\bar{\mathbf{x}}_1 = \sqrt{\eta}\bar{\mathbf{x}}_S$  and same CM  $\mathbf{V}_1 = (\bar{n}_B + 1/2)\mathbf{I}$ .

Note that we have  $\rho_1^{\text{th}} = D(\sqrt{\eta}\alpha)\rho_0^{\text{th}}D(-\sqrt{\eta}\alpha)$  where  $D$  is the phase-space displacement operator.

## QIR performance

In the setting of asymmetric hypothesis testing, the maximum performance achievable by a QIR is given by the quantum Stein's lemma [7, 8]. Suppose we want to discriminate between  $M$  copies of two states,  $\rho_0$  and  $\rho_1$ , using an optimal quantum measurement with output  $k = 0, 1$ . At fixed false-alarm probability  $p_{\text{FA}} := p(1|\rho_0^{\otimes M})$ , we have the following decay of the false-negative (mis-detection) probability

$$p_{\text{MD}} := p(0|\rho_1^{\otimes M}) \simeq \exp(-\beta M), \quad (1)$$

for some rate or error exponent  $\beta$ . According to the quantum Stein's lemma, the optimal rate  $\beta$  is equal to the relative entropy between the two states, i.e.,

$$\beta = D(\rho_0||\rho_1) := \text{Tr}[\rho_0(\ln \rho_0 - \ln \rho_1)]. \quad (2)$$

In a more refined version, we may account for second order asymptotics in  $M$  and write [11]

$$p_{\text{MD}} = e^{-MD(\rho_0||\rho_1) - \sqrt{MV(\rho_0||\rho_1)}\Phi^{-1}(p_{\text{FA}}) + \mathcal{O}(\log M)}, \quad (3)$$

where we also use the quantum relative entropy variance

$$V(\rho_0||\rho_1) = \text{Tr}[\rho_0(\ln \rho_0 - \ln \rho_1)^2] - [D(\rho_0||\rho_1)]^2, \quad (4)$$

and the cumulative distribution function

$$\Phi(\varepsilon) := \frac{1}{\sqrt{2\pi}} \int_{-\infty}^{\varepsilon} dx \exp(-x^2/2), \quad (5)$$

with  $\varepsilon \in (0, 1)$  corresponding to (or bounding) the false-alarm probability  $p_{\text{FA}}$ .

However, we need to notice that the term  $\mathcal{O}(\log M)$  in Eq. (3) may play a non-trivial role in SNR calculations where  $M$  is not so large. According to Theorem 5 of Ref. [11], we have that  $\mathcal{O}(\log M)$  is between 0 and  $2 \log M$ , so that we have upper and lower bounds for  $p_{\text{MD}}$  (with quite some gap). A more refined calculation involves to compute the third moment  $T$  appearing in that theorem. This will give more refined upper and lower bounds for the performance of coherent states.

### First- and second-order terms

We can write explicit formulas for the relative entropy  $D(\rho_0||\rho_1)$  and the relative entropy variance  $V(\rho_0||\rho_1)$  of two arbitrary  $N$ -mode Gaussian states,  $\rho_0(\bar{\mathbf{x}}_0, \mathbf{V}_0)$  and  $\rho_1(\bar{\mathbf{x}}_1, \mathbf{V}_1)$ . The first one is given by [12]

$$D(\rho_0||\rho_1) = -\Sigma(\mathbf{V}_0, \mathbf{V}_0) + \Sigma(\mathbf{V}_0, \mathbf{V}_1), \quad (6)$$

where we have defined the function

$$\Sigma(\mathbf{V}_0, \mathbf{V}_1) = \frac{\ln \det(\mathbf{V}_1 + \frac{i\Omega}{2}) + \text{Tr}(\mathbf{V}_0 \mathbf{G}_1) + \delta^T \mathbf{G}_1 \delta}{2}, \quad (7)$$

with  $\delta = \bar{\mathbf{x}}_0 - \bar{\mathbf{x}}_1$  and  $\mathbf{G}_1 = 2i\Omega \coth^{-1}(2i\mathbf{V}_1\Omega)$  being the Gibbs matrix [13]. The second one is given by [14, 15]

$$V(\rho_0||\rho_1) = \frac{\text{Tr}[(\Gamma \mathbf{V}_0)^2]}{2} + \frac{\text{Tr}[(\Gamma \Omega)^2]}{8} + \delta^T \mathbf{G}_1 \mathbf{V}_0 \mathbf{G}_1 \delta, \quad (8)$$

where  $\Gamma = \mathbf{G}_0 - \mathbf{G}_1$ . Using the output states,  $\rho_0^{\text{th}}$  and  $\rho_1^{\text{th}}$ , it is easy to compute

$$\begin{aligned} D &:= D(\rho_0^{\text{th}}||\rho_1^{\text{th}}) = \eta \bar{n}_S \ln(1 + \bar{n}_B^{-1}) \\ &= \gamma \bar{n}_B \ln(1 + \bar{n}_B^{-1}), \end{aligned} \quad (9)$$

$$\begin{aligned} V &:= V(\rho_0^{\text{th}}||\rho_1^{\text{th}}) = \eta \bar{n}_S (2\bar{n}_B + 1) \ln^2(1 + \bar{n}_B^{-1}) \\ &= \gamma \bar{n}_B (2\bar{n}_B + 1) \ln^2(1 + \bar{n}_B^{-1}), \end{aligned} \quad (10)$$

where  $\gamma := \eta \bar{n}_S / \bar{n}_B$  is the SNR. Note that, for large background noise  $\bar{n}_B \gg 1$ , we can expand

$$D \simeq \gamma + \mathcal{O}(\bar{n}_B^{-1}), \quad V \simeq 2\gamma + \mathcal{O}(\bar{n}_B^{-2}). \quad (11)$$

Following Ref. [11, Theorem 5], we may write the following (approximate) bounds

$$\frac{\Lambda}{M^2} \lesssim p_{\text{MD}} \lesssim \Lambda, \quad (12)$$

where

$$\Lambda := \exp\left[-MD - \sqrt{MV}\Phi^{-1}(p_{\text{FA}})\right]. \quad (13)$$

The upper bound in Eq. (12) is the tool typically used in the literature, while the lower bound is not taken into account (despite the gap between the two bounds can become quite large).

### Computation of the third-order moment

A more accurate version of Eq. (12) includes higher-order terms and suitable conditions of validity. Following Ref. [11], let us introduce the third-order (absolute) moment

$$T(\rho_0||\rho_1) = \sum_{x,y} |\langle a_x | b_y \rangle|^2 \alpha_x \left| \ln \frac{\alpha_x}{\beta_y} - D(\rho_0||\rho_1) \right|^3, \quad (14)$$

where we use the spectral decompositions of the states

$$\rho_0 = \sum_x \alpha_x |a_x\rangle \langle a_x|, \quad \rho_1 = \sum_y \beta_y |b_y\rangle \langle b_y|. \quad (15)$$

See Appendix for more details about the notation behind the formula in Eq. (14).

Let  $0 < C < 0.4748$  be the constant in the Berry–Esseen theorem [16, 17]. Then, we may then write the more accurate bounds [11, Theorem 5]

$$\begin{aligned} \frac{1}{2^9 M^2} \exp\left[-MD(\rho_0||\rho_1) - \sqrt{MV(\rho_0||\rho_1)}\Phi^{-1}(\theta_L)\right] \\ \leq p_{\text{MD}} \leq \\ \exp\left[-MD(\rho_0||\rho_1) - \sqrt{MV(\rho_0||\rho_1)}\Phi^{-1}(\theta_U)\right], \end{aligned} \quad (16)$$

where

$$\theta_L := p_{\text{FA}} + \frac{1}{\sqrt{M}} \left( \frac{CT}{V(\rho_0||\rho_1)^{3/2}} + 2 \right), \quad (17)$$

$$\theta_U := p_{\text{FA}} - \frac{1}{\sqrt{M}} \frac{CT}{V(\rho_0||\rho_1)^{3/2}}. \quad (18)$$

More precisely, the bounds in Eq. (16) are valid as long as  $M$  is large enough to guarantee that  $\theta_L \leq 1$  and  $\theta_U \geq 0$ , so that they fall in the domain of  $\Phi^{-1}$ . From Eq. (16), we can again notice how the lower bound become lose for increasing  $M$ .

Let us compute the third moment  $T$  for the output states  $\rho_0^{\text{th}}$  and  $\rho_1^{\text{th}}$ , associated with the two hypothesis (see Introduction). We have the following number-state spectral decompositions

$$\rho_0^{\text{th}} = \sum_{k=0}^{\infty} \gamma_k |k\rangle \langle k|, \quad \gamma_k := \frac{\bar{n}_B^k}{(\bar{n}_B + 1)^{k+1}}, \quad (19)$$

$$\begin{aligned} \rho_1^{\text{th}} &= D(\sqrt{\eta}\alpha)\rho_0^{\text{th}}D(-\sqrt{\eta}\alpha) \\ &= \sum_{k=0}^{\infty} \gamma_k |k, \sqrt{\eta}\alpha\rangle \langle k, \sqrt{\eta}\alpha|, \end{aligned} \quad (20)$$

whre  $|k, \sqrt{\eta}\alpha\rangle = D(\sqrt{\eta}\alpha)|k\rangle$  is a displaced number state.

Using these decompositions in Eq. (14), we find

$$\begin{aligned} T(\rho_0^{\text{th}}||\rho_1^{\text{th}}) &= \sum_{k,l=0}^{\infty} |\langle k | l, \sqrt{\eta}\alpha \rangle|^2 \gamma_k \left| \ln \frac{\gamma_k}{\gamma_l} - D(\rho_0||\rho_1) \right|^3 \\ &= \sum_{k,l=0}^{\infty} |\langle k | D(\sqrt{\eta}\alpha) | l \rangle|^2 \gamma_k \left| \ln \frac{\gamma_k}{\gamma_l} - D(\rho_0||\rho_1) \right|^3. \end{aligned} \quad (21)$$

Because

$$D(\rho_0^{\text{th}}||\rho_1^{\text{th}}) = \eta \bar{n}_S \ln \left( \frac{\bar{n}_B + 1}{\bar{n}_B} \right), \quad (22)$$

$$\frac{\gamma_k}{\gamma_l} = \frac{\bar{n}_B^{k-l}}{(\bar{n}_B + 1)^{k-l}}, \quad (23)$$

$$\ln \frac{\gamma_k}{\gamma_l} = (k-l) \ln \left( \frac{\bar{n}_B}{\bar{n}_B + 1} \right), \quad (24)$$

we may simplify

$$T(\rho_0^{\text{th}} || \rho_1^{\text{th}}) = \sum_{k,l=0}^{\infty} |\langle k | D(\sqrt{\eta}\alpha) | l \rangle|^2 \quad (25)$$

$$\times \gamma_k \left| (k-l + \eta\bar{n}_S) \ln \left( \frac{\bar{n}_B}{\bar{n}_B + 1} \right) \right|^3.$$

Now recall that [18, Eq. (3.30) and Appendix B]

$$\langle k | D(\alpha) | l \rangle = \sqrt{\frac{l!}{k!}} \alpha^{k-l} e^{-|\alpha|^2/2} \mathcal{L}_l^{(k-l)}(|\alpha|^2), \quad (26)$$

where  $\mathcal{L}_n^{(m)}(x)$  is an associated Laguerre polynomial, which takes the following form in terms of the binomial coefficient [19]

$$\mathcal{L}_n^{(m)}(x) := \sum_{k=0}^n \binom{n+m}{n-k} \frac{(-x)^k}{k!}. \quad (27)$$

Therefore, for  $\bar{n}_S = |\alpha|^2$ , we may compute

$$|\langle k | D(\sqrt{\eta}\alpha) | l \rangle|^2 = \frac{l!}{k!} (\eta\bar{n}_S)^{k-l} e^{-\eta\bar{n}_S} \left[ \mathcal{L}_l^{(k-l)}(\eta\bar{n}_S) \right]^2, \quad (28)$$

so that we find the analytical expression

$$T(\rho_0^{\text{th}} || \rho_1^{\text{th}}) = e^{-\eta\bar{n}_S} \sum_{k,l=0}^{\infty} \frac{l!}{k!} \gamma_k (\eta\bar{n}_S)^{k-l} \left[ \mathcal{L}_l^{(k-l)}(\eta\bar{n}_S) \right]^2$$

$$\times \left| (k-l + \eta\bar{n}_S) \ln \left( \frac{\bar{n}_B}{\bar{n}_B + 1} \right) \right|^3. \quad (29)$$

Note that this expression can be put in terms of the SNR  $\gamma = \eta\bar{n}_S/\bar{n}_B$  and the thermal background  $\bar{n}_B$ , i.e., we may equivalently write

$$T(\rho_0^{\text{th}} || \rho_1^{\text{th}}) = e^{-\gamma\bar{n}_B} \sum_{k,l=0}^{\infty} \frac{l!}{k!} \gamma_k (\gamma\bar{n}_B)^{k-l} \left[ \mathcal{L}_l^{(k-l)}(\gamma\bar{n}_B) \right]^2$$

$$\times \left| (k-l + \gamma\bar{n}_B) \ln \left( \frac{\bar{n}_B}{\bar{n}_B + 1} \right) \right|^3. \quad (30)$$

Furthermore, suitable bounds might be used for the Laguerre polynomials (see Appendix ).

### Numerical investigation

In order to perform a numerical comparison, we consider the error exponent

$$\varepsilon_{\text{MD}} := \frac{-\ln p_{\text{MD}}}{M}, \quad (31)$$

which corresponds to  $\beta$  in Eq. (1) at the first order. It is clear that the higher is the value of  $\varepsilon_{\text{MD}}$ , the better is the discrimination performance.

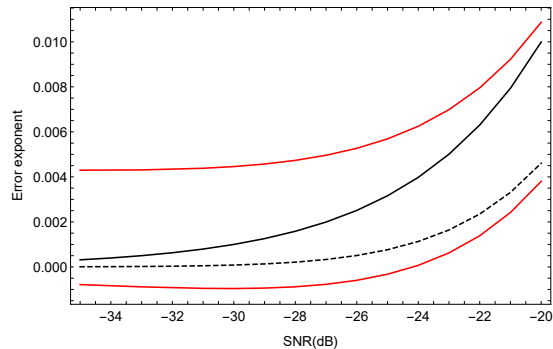


FIG. 1: Error exponent  $\varepsilon_{\text{MD}}$  as a function of the SNR in dBs  $10 \log_{10} \gamma$ . We compare the first order approximation of Eq. (1) (black line), with the higher-order lower and upper bounds from Eq. (16) (red lines). We also plot the Marcum benchmark (dashed black line). We consider the parameters  $p_{\text{FA}} = 10^{-3}$ ,  $M = 5000$  and  $\bar{n}_B = 600$ . Note that the lower bound even becomes negative for lower values of SNRs.

To show the finite-size behavior, we consider  $p_{\text{FA}} = 10^{-3}$ ,  $M = 5000$  and bright background  $\bar{n}_B = 600$ . With these parameters, we plot  $\varepsilon_{\text{MD}}$  versus SNR in decibels (i.e.,  $10 \log_{10} \gamma$ ) for the optimized detection for coherent states considering the first order formula of Eq. (1), and the higher-order bounds in Eq. (16). As a comparison, we also plot the error exponent achievable by a classical radar which employs coherent state pulses and heterodyne detection [1]. This can be computed from the Marcum Q-function [20, 21]

$$p_{\text{MD}} = 1 - Q\left(\sqrt{2\gamma}, \sqrt{-2 \ln p_{\text{FA}}}\right), \quad (32)$$

$$Q(x, y) := \int_y^\infty dt t e^{-(t^2+x^2)/2} I_0(tx), \quad (33)$$

with  $I_0(\cdot)$  being the modified Bessel function of the first kind of zero order.

As we can see from Fig. 1, the QIR would have a clear advantage over the Marcum benchmark if we consider the asymptotic first order formula. However, the first order expression of Eq. (1) is valid only for very large  $M$ . For a typical finite size value of  $M$ , we need to consider the higher-order bounds in Eq. (16), but we see that the gap is too large to reach a conclusion of quantum advantage.

### Conclusion

In this work, we have studied a quantum-inspired lidar/radar based on coherent states and optimal quantum detection, analysing the performance in the context of asymmetric hypothesis testing (quantum Stein's lemma, higher-order asymptotics). According to our study, the current mathematical tools do not allow us to prove quantum advantage over classical strategies based on coherent states and heterodyne detection when a finite

number of probes is considered. Such an advantage may be claimed in the asymptotic limit of very large number of probes, so that the first order order becomes completely dominant over the higher-order terms. However, such an asymptotic regime is not relevant for practical applications.

**Acknowledgments.** This work has been funded by the European Union's Horizon 2020 Research and Innovation Action under grant agreement No. 862644 (FE-TOpen project: Quantum readout techniques and technologies, QUARTET). S. P. would like to thank Quntao Zhuang for discussions.

- 
- [1] I. S. Merrill *et al.*, *Introduction to radar systems* (McGraw-Hill, 1981).
- [2] S. Lloyd, *Enhanced sensitivity of photodetection via quantum illumination*, *Science* **321**, 1463-1465 (2008).
- [3] S. Pirandola and S. Lloyd, *Computable bounds for the discrimination of Gaussian states*, *Phys. Rev. A* **78**, 012331 (2008).
- [4] S.-H. Tan *et al.*, *Quantum illumination with Gaussian states*, *Phys. Rev. Lett.* **101**, 253601 (2008).
- [5] S. Barzanjeh *et al.*, *Microwave quantum illumination*, *Phys. Rev. Lett.* **114**, 080503 (2015).
- [6] S. Pirandola, B. Roy Bardhan, T. Gehring, C. Weedbrook, and S. Lloyd, *Advances in Photonic Quantum Sensing*, *Nat. Photon.* **12**, 724-733 (2018).
- [7] F. Hiai and D. Petz, *The proper formula for relative entropy and its asymptotics in quantum probability*, *Commun. Math. Phys.* **143**, 99-114 (1991).
- [8] T. Ogawa and H. Nagaoka, *Strong converse and Stein's lemma in quantum hypothesis testing*, *Asymptotic Theory Of Quantum Statistical Inference: Selected Papers*, 28-42 (World Scientific, 2005).
- [9] K. M. R. Audenaert, M. Nussbaum, A. Szkola, and F. Verstraete, *Asymptotic Error Rates in Quantum Hypothesis Testing*, *Commun. Math. Phys.* **279**, 251 (2008).
- [10] G. Spedalieri and S. L. Braunstein, *Asymmetric quantum hypothesis testing with Gaussian states*, *Phys. Rev. A* **90**, 052307 (2014).
- [11] K. Li, *Second-order asymptotics for quantum hypothesis testing*, *Annals of Statistics* **42**, 171-189 (2014).
- [12] S. Pirandola, R. Laurenza, C. Ottaviani, and L. Banchi, *Fundamental Limits of Repeaterless Quantum Communications*, *Nat. Commun.* **8**, 15043 (2017). See also arXiv:1510.08863 (2015).
- [13] L. Banchi, S. L. Braunstein, and S. Pirandola, *Quantum fidelity for arbitrary Gaussian states*, *Phys. Rev. Lett.* **115**, 260501 (2015).
- [14] S. Pirandola, U. L. Andersen, L. Banchi, M. Berta, D. Bunandar, R. Colbeck, D. Englund, T. Gehring, C. Lupo, C. Ottaviani, J. Pereira, M. Razavi, J. S. Shaari, M. Tomamichel, V. C. Usenko, G. Vallone, P. Villoresi, and P. Wallden, *Advances in Quantum Cryptography*, *Adv. Opt. Photon.* **12**, 1012-1236 (2020).
- [15] M. M. Wilde, M. Tomamichel, S. Lloyd, and M. Berta, *Gaussian hypothesis testing and quantum illumination*, *Phys. Rev. Lett.* **119**, 120501 (2017).
- [16] V. Y. Korolev and I. G. Shevtsova, *On the upper bound for the absolute constant in the Berry-Esseen inequality*, *Theory of Probability & Its Applications*, 54, 638-658 (2010).
- [17] I. Shevtsova, *On the absolute constants in the Berry-Esseen type inequalities for identically distributed summands*, arXiv:1111.6554 (2011).
- [18] K. E. Cahill and R. J. Glauber, *Ordered Expansions in Boson Amplitude Operators*, *Phys. Rev.* **177**, 1857 (1969).
- [19] G. Szegő, *Orthogonal Polynomials*, Amer. Math. Soc. Colloq. Publ. 23, Amer. Math. Soc., Providence, RI, fourth edition, 1975.
- [20] J. I. Marcum, *A Statistical Theory of Target Detection by Pulsed Radar: Mathematical Appendix*, RAND Corporation, Santa Monica, CA, Research Memorandum RM-753, July 1, 1948. Reprinted in IRE Transactions on Information Theory **IT-6**, 59-267 (1960).
- [21] W. Albersheim, *A closed-form approximation to Robertson's detection characteristics*, *Proc. of the IEEE* **69**, 839-839 (1981).
- [22] M. Nussbaum, and A. Szkola, *The Chernoff lower bound for symmetric quantum hypothesis testing*, *Ann. Statist.* **37**, 1040-1057 (2009).
- [23] P. G. Rooney, *Further inequalities for generalized Laguerre polynomials*, *C.R. Math. Rep. Acad. Sci. Canada* **7**, 273-275 (1985).

### Relative entropy notation [22]

Relative entropy is given by

$$D(\rho_0||\rho_1) := \text{Tr}[\rho_0(\ln \rho_0 - \ln \rho_1)]. \quad (34)$$

Using the spectral decompositions

$$\rho_0 = \sum_x \alpha_x |a_x\rangle \langle a_x|, \quad \rho_1 = \sum_y \beta_y |b_y\rangle \langle b_y|, \quad (35)$$

and therefore

$$\ln \rho_0 = \sum_x \ln \alpha_x |a_x\rangle \langle a_x|, \quad (36)$$

$$\ln \rho_1 = \sum_y \ln \beta_y |b_y\rangle \langle b_y|, \quad (37)$$

we may write

$$D(\rho_0||\rho_1) = \sum_x \alpha_x \langle a_x | (\ln \rho_0 - \ln \rho_1) | a_x \rangle \quad (38)$$

$$= \sum_x \alpha_x \left[ \ln \alpha_x - \sum_y \ln \beta_y |\langle a_x | b_y \rangle|^2 \right]. \quad (39)$$

Let us set  $|a_x\rangle = \sum_y \gamma_{xy} |b_y\rangle$  with complex  $\gamma_{xy}$  such that  $\sum_x |\gamma_{xy}|^2 = \sum_y |\gamma_{xy}|^2 = 1$ . Therefore,

$$\begin{aligned} D(\rho_0||\rho_1) &= \sum_x \alpha_x \left( \ln \alpha_x - \sum_y \ln \beta_y |\gamma_{xy}|^2 \right) \\ &= \sum_{x,y} \alpha_x |\gamma_{xy}|^2 (\ln \alpha_x - \ln \beta_y) \\ &= \sum_{x,y} p_{xy} \ln \frac{\alpha_x}{\beta_y} := \left\langle \ln \frac{\alpha(X)}{\beta(Y)} \right\rangle, \end{aligned} \quad (40)$$

where  $\alpha(X) := \{\alpha_x, p_x\}$ ,  $\beta(Y) := \{\beta_y, p_y\}$  where  $p_x$  and  $p_y$  are the marginal distributions of the joint probability  $p_{xy} := \alpha_x |\gamma_{xy}|^2$  which is the probability to get  $X = x$  and  $Y = y$  by measuring  $\rho_0$  in the basis  $\{|a_x\rangle\}$  and then in  $\{|b_y\rangle\}$ . In this notation, we may also write the relative entropy variance as follows

$$V(\rho_0||\rho_1) = \left\langle \ln \frac{\alpha(X)}{\beta(Y)} \right\rangle^2 - D(\rho_0||\rho_1)^2. \quad (41)$$

The third-order moment entering the quantum Stein's lemma is given by [11]

$$\begin{aligned} T(\rho_0||\rho_1) &= \left\langle \left| \ln \frac{\alpha(X)}{\beta(Y)} - D(\rho_0||\rho_1) \right|^3 \right\rangle \\ &= \sum_{x,y} |\langle a_x | b_y \rangle|^2 \alpha_x \left| \ln \frac{\alpha_x}{\beta_y} - D(\rho_0||\rho_1) \right|^3. \end{aligned} \quad (42)$$

$$(43)$$

## Useful bounds

Various bounds are known for the associated Laguerre polynomials. A well-known uniform bound is the Szegö bound [19]

$$\left| \mathcal{L}_n^{(m)}(x) \right| \leq \frac{(m+1)_n}{n!} e^{x/2}, \quad (44)$$

for  $x, m \geq 0$ ,  $n = 0, 1, \dots$  where we use the Pochhammer's symbol (or shifted factorial)

$$(a)_0 = 1, \quad (45)$$

$$(a)_n = a(a+1)(a+2)\cdots(a+n-1), \quad (46)$$

$$(a)_n = \frac{\Gamma(a+n)}{\Gamma(a)} \quad (47)$$

with  $\Gamma(a)$  being the Gamma function. Another one is [23]

$$\left| \mathcal{L}_n^{(m)}(x) \right| \leq 2^{-m} q_n e^{x/2}, \quad (48)$$

for  $x \geq 0$ ,  $m \leq -1/2$ ,  $n = 0, 1, \dots$  and where we set

$$q_n = \frac{\sqrt{(2n)!}}{2^{n+1/2} n!} \simeq \frac{1}{\sqrt[4]{4\pi n}} \text{ for large } n. \quad (49)$$